

Improved region growing segmentation for breast cancer detection: progression of optimized fuzzy classifier

Segmentation
for breast
cancer
detection

181

Rajeshwari S. Patil

*Department of Electronics and Communication,
BLDEA's V P Dr PG Halakatti College of Engineering and Technology,
Bijapur, India, and*

Nagashettappa Biradar

*Department of Electronics and Communication,
Bheemanna Khandre Institute of Technology, Bidar, India*

Received 30 October 2019
Revised 8 February 2020
Accepted 10 February 2020

Abstract

Purpose – Breast cancer is one of the most common malignant tumors in women, which badly have an effect on women's physical and psychological health and even danger to life. Nowadays, mammography is considered as a fundamental criterion for medical practitioners to recognize breast cancer. Though, due to the intricate formation of mammogram images, it is reasonably hard for practitioners to spot breast cancer features.

Design/methodology/approach – Breast cancer is one of the most common malignant tumors in women, which badly have an effect on women's physical and psychological health and even danger to life. Nowadays, mammography is considered as a fundamental criterion for medical practitioners to recognize breast cancer. Though, due to the intricate formation of mammogram images, it is reasonably hard for practitioners to spot breast cancer features.

Findings – The performance analysis was done for both segmentation and classification. From the analysis, the accuracy of the proposed IAP-CSA-based fuzzy was 41.9% improved than the fuzzy classifier, 2.80% improved than PSO, WOA, and CSA, and 2.32% improved than GWO-based fuzzy classifiers. Additionally, the accuracy of the developed IAP-CSA-fuzzy was 9.54% better than NN, 35.8% better than SVM, and 41.9% better than the existing fuzzy classifier. Hence, it is concluded that the implemented breast cancer detection model was efficient in determining the normal, benign and malignant images.

Originality/value – This paper adopts the latest Improved Awareness Probability-based Crow Search Algorithm (IAP-CSA)-based Region growing and fuzzy classifier for enhancing the breast cancer detection of mammogram images, and this is the first work that utilizes this method.

Keywords Mammogram, Breast cancer detection, Optimized region growing, Membership optimized-fuzzy classifier, Improved crow search algorithm

Paper type Research paper

Nomenclatures

GLRM	Gray-Level Run-Length Matrix	KNN	K Nearest Neighbour
LGRE	Low Grey Level Run Emphasis	RBFSVM	Radial Basis Function Support
CSA	Crow Search Algorithm		Vector Machine
MRI	Magnetic Resonance Imaging	ROI	Region of Interest
PET	Positron Emission Tomography	FrCN	Full resolution Convolutional
CNN	Convolutional Neural Network		Network
FDR	False Discovery Rate	MCC	Mathews Correlation Coefficient
SVM	Support Vector Machine	DL-CNN	Deep Learning Convolutional
FNR	False Negative Rate		Neural Network
2D	Two Dimensional	VGGNet	Visual Geometry Group Network



ResNet	Residual Networks	NPV	Negative Predictive Value
GLCM	Gray-Level Co-occurrence Matrix	DT	Decision Tree
HGRE	High Grey Level Run Emphasis	DDSM	Digital database for screening mammography
FPR	False Positive Rate		
NN	Neural Network		

1. Introduction

Breast cancer is a wide-spread type of cancer, which is strangely affecting women (Jasbi *et al.*, 2019). Breast cancer is ranking second, which became the most common disease after lung cancer (Siegel *et al.*, 2018). Early avoidance of breast cancer is not possible because the reason of causing is not clear. It is reported that there is a chance for a patient to survive if the cancer is recognized in the starting stage (Oliveira *et al.*, 2011). In general, screening and detection of cancer are mostly done in the last stages due to a lack of proper awareness. Especially due to lack of funds, in some countries, breast cancer screening programs have not been arranged yet. The use of imaging has assisted in the detection and localization of infectious tissues for biopsy, recognition of metastasis, biopsy and medical care protocol plans (Menegaz and Guimarães, 2019). Few techniques are adopted to distinguish organs and tissues for assisting the detection of abnormalities such as tumors, ultrasonography (Qi *et al.*, 2019), MRI (Herent *et al.*, 2019), PET (Kim *et al.*, 2019), tomosynthesis (Osman *et al.*, 2018) and mammography for breast cancer.

In the current scenario, early diagnosis of breast cancer has successfully happened through mammography, which identifies the abnormalities before the patients attack with the specified symptoms. Mammography can easily recognize breast cancer by revealing a patient's breast to the low extent of X-ray radiation as there are diverse X-ray absorption rates among abnormal and normal tissues. In general, tumors in mammogram images are represented as masses or any abnormal growth (Poorolajal *et al.*, 2017). Breast tomosynthesis was approved as the new mammography technique by FDA. By considering several photographs of X-ray from various angles and making the images into a video, the tomosynthesis gives further assistance to radiologists in finding the peculiarities as it keeps away from the surface of dense tissue and tumor mass (Kopans, 2013). Even though mammography-based screening has been performed to decrease the deaths caused due to breast cancer, high false-positive results and high recall rates are connected with mammography to avoid potential mass diagnosis (Hellquist *et al.*, 2010; Nelson *et al.*, 2016).

The pros and cons of early diagnosis of breast cancer have been motivated to develop an automatic model for helping the radiologist expert in improving the interpretation accuracy. To improvise the classifiers, CNN-based models (Fan *et al.*, 2019) are merged with the techniques such as transfer learning (Hellquist *et al.*, 2010) and data augmentation (Kopans, 2013). Moreover, for attaining the best performance by integrating several base estimators, ensemble approaches are utilized. Different methods are there for weight updating in AdaBoost (Freund and Schapire, 1997), classification by NN and AdaBoost with DT as a base estimator is executed, and the report is generated based on the performance of AdaBoost. (Kuncheva and Whitaker, 2002; Dietterich, 2000; Schwenk and Bengio, 2000). Still, there is a prerequisite to finding a new way of diagnosing breast cancer to achieve high accuracy.

The main intention of the paper is as follows:

- (1) It includes four phases: image pre-processing, tumor segmentation, extracting features and detection. In pre-processing, the noise is removed using a median filter, which enhances the image.
- (2) The optimized region growing algorithm is adopted for lesion segmentation, where the tolerance is optimized by a new modified algorithm called IAP-CSA. This is done

by fixing the objective as maximizing the segmentation accuracy when compared with the ground truth image. Two sets of features like GLCM and GLRM are extracted in the feature extraction phase from segmented images.

- (3) Finally, the classification procedure is performed by the modified Fuzzy Logic classifier to classify the image into three classes, such as normal, benign, and malignant. The modification is done by optimizing the membership function of the Fuzzy Logic classifier using proposed IAP-CSA to maximize the detection accuracy.

The entire paper is designed in the following manner: [Section 2](#) specifies the literature review and the features and challenges of conventional approaches for detecting breast cancer automatically. Pre-processing and segmentation embraced in the proposed breast cancer detection model is shown in [Section 3](#). Proposed breast cancer detection model: An optimized fuzzy classifier with the proposed objective model is shown in [Section 4](#). Finally, results and discussions are seen in [Section 5](#); final comments are given in [Section 6](#).

2. Literature review

2.1 Related works

[Vijayarajeswari et al. \(2019\)](#) had conferred classification of the mammogram by feature extraction using two-dimensional transform known as Hough transform, which was used to separate features of appropriate shape in an image. As the masses were frequently not defined from the computerized mass location, encompassing parenchymal, and adjustment was more difficult. Moreover, the Hough transform was utilized to recognize the mammogram features, and it was categorized by SVM. The suggested method was tested on 95 mammogram images gathered and categorized. The classification accuracy was improved with the SVM classifier. Hence, the resultant of the recommended approach was efficient in distinguishing the mammograms, abnormal classes.

[Zhang et al. \(2018\)](#) have suggested a method of mammogram and tomosynthesis detection depending on CNNs. From the University of Kentucky, 3,000 tomosynthesis and mammograms data was collected for experimenting with the proposed system. Various designs of CNNs were framed to organize 3D tomosynthesis, and 2D mammograms and the truth values obtained from the biopsy were considered for each classifier. Finally, the output verified that the CNN-based approach was optimized using transfer learning and data expansion, which has a well prospective for automatic detection of breast cancer.

[Li et al. \(2019\)](#) have recommended an enhanced DenseNet NN model to obtain an accurate and robust classification of malignant and benign mammography images. At first, the input images were pre-processed. The pre-processed mammogram datasets were given as inputs to AlexNet, VGGNet, DenseNet-II NN, DenseNet Network model, and GoogLeNet approach, and the test outcomes were evaluated and contrasted. Moreover, the results revealed that the DenseNet-II NN approach has improved performance based on the 10-fold validation method when compared with the rest of the network approaches. The analysis of accuracy proved that the proposed system is effective for classifying the mammogram images into benign and malignant.

[Bhosle and Deshmukh \(2018\)](#) have proposed the Hybrid KNN-RBFSVM algorithm for breast cancer detection. At first, identical weights were allocated to every mammogram, and modernized weights were originated. For the RBFSVM model, the improved weights were utilized as the first weights. The proposed algorithm was used as a base estimator in AdaBoost by 200 estimators to predict the test mammogram as benevolent or malevolent. Further, from mammograms, the GLCM features were taken, and the mammogram features influence the detection accuracy. In the classification part, AdaBoost was used, and the obtained results were contrasted with KNN, Hybrid KNN-RBFSVM, and DT by analyzing

measures like ROC curve and accuracy. For the simulation, the DDSM mammogram image dataset was utilized, and the results revealed that AdaBoost with the proposed system had attained the best accuracy and AUC over ensemble approaches.

Seryasat and Haddadnia (2018) have carried out a computer-aided mechanism for mammogram images to classify benign and malignant types. By using a robust noise removal approach, the noise present in the mammograms was decreased. Next, the mass in the ROI was segmented by a deformable model. The feature extraction process was started further, which consists of the characteristics of mass shape and border, fractal dimension, and the properties of tissue. Once pulling out a bulk amount of characteristics, a real subset was selected from them. In order to select a proper set of features, a new approach was utilized based on the Genetic Algorithm. A classifier was trained after establishing suitable characteristics. Moreover, a new hybrid model was introduced with the combination of classifiers to classify the data, from which simple and tough samples were recognized and trained by distinct classifiers. At last, the developed model has experimented on DDSM and mini-MIAS databases, where the outcomes have shown that the developed model outperforms the existing models.

Al-antari *et al.* (2018) have introduced an FrCN; a new deep network model was proposed to segment the mass. To categorize the mass as either malignant or benign, deep CNN was utilized. To validate the suggested integrated CAD system based on the accuracies of segmentation, classification, and detection, the widely accessible and interpreted INbreast database was used. Then, the extracted masses were categorized by CNN and acquired the accuracy of 95.64%. From the results, it was concluded that the suggested CAD was used to help the radiologists in each and every stage of detection, classification, and segmentation.

Duraisamy and Emperumal (2017) had established a deep learning-based to classify the digital mammograms. This method was depended on deep learning mechanisms, which note the existence of the tumor tissues. It was complicated to steadily segment input image, because of fewer differences between normal and lesion tissues. To extract the mammogram features, the Chan-Vese level set was utilized, and to memorize the characteristics of the mammary-specific mass and microcalcification clusters, DL-CNN was used. For improving the classification accuracy and decreasing the false positives, a fully complex-valued network classifier was exploited to continue the final phase of DL-CNN. Finally, the test results exhibited that the introduced method has great performance enhancement when compared to existing approaches.

Khan *et al.* (2019) have offered a deep learning framework to recognize and categorize breast cancer in breast cytology images by assuming transfer learning. Deep learning architectures were designed to be risk determination and were executed in segregation. Converse to classical learning concepts, which increase and defer in separation, transfer learning was intended to employ the absorbed information in the result of one crisis into other associated crises. Also, the features were taken from pre-trained CNN images, explicitly VGGNet, ResNet, and GoogleNet were given to a fully connected layer for distinguishing the benign and malignant cells by the classification based on average pooling. Finally, the tests were executed on standard benchmark datasets, from which, it has been concluded that the suggested deep learning framework has attained high detection accuracy.

2.2 Review

Even though there are many ways to improve the diagnosis of breast cancer detection, there still exist a few conflicts that need to be solved and progressed. Table 1 specifies some of the merits and drawbacks of state-of-the-art breast cancer detection approaches. Among them, SVM (Vijayarajeswari *et al.*, 2019) has some advantages like high accuracy; it delivers a distinctive solution; and it has high computational speed and memory. Still, it has to enhance

Authors [citations]	Methodology	Features	Challenges
Vijayarajeswari <i>et al.</i> (2019)	Support Vector Machine	(1) It has high accuracy (2) It delivers a distinctive solution (3) It has high computational speed and memory	(1) The performance is low when compared to deep learning algorithms (2) It is difficult to identify tumor cells (3) The segmentation of pectoral muscle need to be extracted
Zhang <i>et al.</i> (2018)	Deep Convolutional Neural Network	(1) They accumulate high complex patterns using smaller or simpler patterns (2) It has high accuracy	(1) Hyperparameter tuning is insignificant (2) Requires a large data set (3) The efficiency of automated ultrasonography image diagnosis should be improved
Li <i>et al.</i> (2019)	DenseNet neural network	(1) The speed of the calculation and efficiency of the network model are improved (2) Can learn easily to combine the various activations, which lead to exact classification	(1) It is often very computationally expensive (2) The speed and efficiency of the network are low
Bhosle and Deshmukh (2018)	KNN + RBFSVM	(1) Tough to noisy training data (2) If the training data is high, then the result will be effective	(1) KNN computational cost is extremely high as the distance of each query need to be computed to all the training samples (2) SVM has many key parameters that need to set exactly to attain the best classification outcome for any difficulty (3) Inconsistent and irrelevant features of mammogram affect the classification accuracy
Seryasat and Haddadnia (2018)	Ensemble learning	(1) Unite the decisions from multiple models to enhance the overall performance (2) They are improbable to overfit	(1) It experiences the requirement of interpretability (2) Generally, they are expensive (3) In mammograms, the noise should be reduced
(continued)			

Table 1.
Features and
challenges of
conventional breast
cancer detection
models

Authors [citations]	Methodology	Features	Challenges
Al-antari et al. (2018)	Full resolution convolutional network	(1) Improves overall performance (2) It can assist radiologists in detection, segmentation, and classification (3) Easy to implement	(1) Requires more training samples (2) It needs an integrated CAD system to screen digital X-ray mammograms involving detection, segmentation, and classification of breast masses
Duraissamy and Emperumal (2017)	Fully Complex-valued Relaxation Network	(1) It has high accuracy (2) It requires less computational effort during training	(1) Need to improve in classification (2) The development of this methodology should be improved to identify tumor tissues (3) It is difficult to segment mammogram image robustly
Khan et al. (2019)	Convolutional Neural Network	(1) It has high accuracy (2) It automatically detects the major features on its own	(1) Need to improve the classification accuracy (2) It has a high computational cost (3) The size of the dataset should be increased to improve the efficiency of CNN structure. (4) It is very difficult to analyze the microscopic images manually due to the irregular appearance of benign and malignant cells.

Table 1.

the performance when compared to deep learning algorithms, and it is difficult to identify tumor cells and needs to extract the segmentation of pectoral muscle. Deep CNN ([Zhang et al., 2018](#)) has accuracy and can accumulate high complex patterns using smaller or simpler patterns. Though there are some disadvantages like hyperparameter tuning which is insignificant, and requires a large amount of dataset, it needs to improve the efficiency of automated ultrasonography images. DenseNet neural network ([Li et al., 2019](#)) can easily learn to combine the various activations, which lead to providing exact classification, as well as the speed of the calculation and efficiency of the network model is improved. Yet, it is often very computationally expensive, and the dataset is avoided and the speed of the network is low. KNN + RBFSVM ([Bhosle and Deshmukh, 2018](#)) are very tough to noisy training data, and if training data is high, then the resultant outcome will be effective. But, there are a few challenges such as its computational cost is extremely high as distance of each query need to be computed to all the training samples, and it has many key parameters needed to set exactly to attain the best classification outcome for any difficulty; the classification accuracy is affected due to inconsistent and irrelevant features of mammogram. Ensemble learning ([Seryasat and Haddadnia, 2018](#)) is improbable to overfit and unites the decisions from multiple models to enhance the overall performance. However, it experiences the requirement of interpretability, and generally, they are expensive and the noise should be reduced in mammograms and the breast cancer rate has increased. FrCN ([Al-antari et al., 2018](#)) is easy to

implement, improves the overall performance, and can assist radiologists in detection, segmentation, and classification. But, it requires more training samples, and it needs an integrated CAD system to screen digital X-ray mammograms involving detection, segmentation and classification of breast masses. FCRN (Duraismy and Emperumal, 2017) has high accuracy, and it requires less computational effort during training. Still, it needs to improve in classification and also needs to improve development methodology, so it is easy to identify tumor tissues, and the contrast is low between normal, and lesion tissues, and it is difficult to segment mammogram images robustly. CNN (Khan *et al.*, 2019) also attains high accuracy, and it automatically detects the major features by their own, yet it suffers from high computational cost and to improve the efficiency of CNN structure the size of dataset should be improved, and the microscopic images are difficult to analyze due to the irregular appearance of benign and malignant cells. Hence, these limitations need to be considered to improve breast cancer detection in the future by developing more effective and beneficial diagnostic models.

3. Preprocessing and segmentation embraced in proposed breast cancer detection model

3.1 Image description

In the current breast cancer diagnosis system, a mammogram image is taken for processing. Let V_m is considered as the input mammogram image. Since the system involves pre-processing, segmentation, and feature extraction phases before classification $V_{m(\text{pre})}$ is considered as a pre-processed image $V_{m(\text{seg})}$ is considered as segmented tumor image, and S_u refers to the extracted features, where $u = 1, 2, \dots, N_U$, and N_U is the number of features extracted, which is later applied to optimized fuzzy classifier for diagnosing breast cancer.

3.2 Preprocessing phase

In image processing, filters are generally adopted to remove the noise from the image by suppressing the low frequencies or high frequencies, which thus improves or detects the edges in the image. For the mammogram image, median filtering (Zhu and Huang, 2012) is used here, which is a nonlinear filter. The main principle of the median filter is to replace the noisy pixels by the median value of neighborhood pixels, sorted based on the gray level of the image. If the median filter is applied for the input image V_m , the output $V_{m(\text{pre})}$ is formulated based on the expression given in equation (1).

$$V_{m(\text{pre})}(x, y) = \text{med}\{V_m(x - j, y - k)j, k \in J\} \quad (1)$$

According to equation (3), V_m refers to the input image, $V_{m(\text{pre})}$ refers to the output image, respectively, and J indicates the 2D mask. Thus after median filtering, $V_{m(\text{pre})}$ is generated, which is taken as the pre-processed image.

3.3 Optimized region growing-based segmentation

The pre-processed image is further subjected for the segmentation process to segment the tumor from the image. Here, the optimized region growing is used, which is the modified version of the single seed region growing algorithm (Feng *et al.*, 2018). For various image segmentations, seeded region growing is broadly utilized. This algorithm operates based on clustering the target pixels into significant image regions. Here, the segmentation of the image is accomplished using a seed pixel, and further continuously join the fresh homogeneous pixels to the seed until the segmentation process is fulfilled on the enlarged segment.

Consider A as the entire area of the input image $V_{m(\text{pre})}$, which is split into c sub-regions A_1, A_2, \dots, A_c . During the region growing algorithm, the following conditions should be satisfied.

- (1) $\cup_{i=1}^c A_i = A$;
- (2) For A_1, A_2, \dots, A_c , A refers to the connected region;
- (3) For any $i, j, i \neq j, A_i \cap A_j = \emptyset$;
- (4) $P(A_i) = \text{true}$
- (5) $A(A_i \cup A_j) = \text{false}$

In the above conditions, $P(A_i)$ indicates the gray level value of the set A_i , and c specifies the total sum of pixels of an image. As mentioned earlier, the selection of seed points is the initial step of the seeded region growing algorithm. Each step of the algorithm includes the inclusion of one pixel to the above set, when the value of the pixels involves the condition shown in [equation \(3\)](#).

$$l = \frac{1}{c} \sum_{(x,y) \in A} g(x,y) \quad (2)$$

$$|g(x,y) - l|_{(x,y) \in A} < \delta \quad (3)$$

The average of the image l is represented in [equation \(2\)](#), where $g(x,y)$ indicates the value at the coordinate (x,y) . Moreover, the term δ is defined as tolerance or threshold, which should be nearer to the average of the image.

According to the working strategy of this algorithm, the selection of seed and tolerance δ plays a fundamental role in enhancing the segmentation performance. The conventional seeded region growing algorithm needs the human effort to select these parameters, which commence the subjective elements, and demands the exact tuning of parameters. To achieve robust automatic segmentation, the tolerance of the seeded region growing algorithm is tuned or optimized with the aid of proposed IAS-CSA that should be between 0 and 256.

3.4 Extraction of GLCM and GLRM features

After the tumor segmentation, two sets of features like GLCM, and GLRM is extracted, which is clearly formulated below.

GLCM ([Malegori et al., 2016](#)): It is a method to compute the texture features by considering the spatial relationship of pixels. In general, this approach assesses the possibility of pairs of pixels with certain values, which helps to observe the spatial relationship in an image. The formulation for energy is given in [equation \(4\)](#), where G_{ij} specifies the $(i,j)^{\text{th}}$ element in the normalized GLCM.

$$\text{EN} = \sum_i \sum_j G_{ij}^2 \quad (4)$$

Moreover, the mathematical formula for contrast, entropy, and homogeneity is given in [equations \(5\), \(6\), and \(7\)](#), respectively.

$$\text{CN} = \sum_i \sum_j (i - j)^2 G_{ij} \quad (5)$$

$$EY = -\sum_i \sum_j G_{ij} \log_2 G_{ij} \quad (6) \quad \text{Segmentation for breast cancer detection}$$

$$HM = \sum_i \sum_j \frac{1}{1 + (i-j)^2} G_{ij} \quad (7)$$

Similarly, the variance is determined based on [equation \(8\)](#), where μ refers to the mean of G_{ij} . [Equation \(9\)](#) shows the sum average, and [equation \(10\)](#) shows the correlation.

189

$$VR = \sum_i \sum_j (i - \mu)^2 G_{ij} \quad (8)$$

$$SA = \sum_{i=2}^{2N_f-2} i G_{x+y}(i) \quad (9)$$

$$CR = \frac{\sum_i \sum_j (i \times j) G_{ij} - \mu_x \mu_y}{\sigma_x \sigma_y} \quad (10)$$

In [equation \(9\)](#) and [equation \(10\)](#), N_f indicates the number of gray level in image, μ_x and μ_y denote the mean of G_x and G_y , respectively, and σ_x σ_y denote the standard deviation of G_x and G_y , respectively. [Equation \(11\)](#) to [equation \(16\)](#) represent the sum variance, sum entropy, difference entropy, difference variance, information measures of correlation (IMC1, IMC2) and maximum correlation coefficient, respectively.

$$SV = \sum_{i=2}^{2N_f} (i - SA)^2 G_{x+y}(i) \quad (11)$$

$$SE = \sum_{i=2}^{2N_f} G_{x+y}(i) \log \{G_{x+y}(i)\} \quad (12)$$

$$DE = \sum_{i=0}^{N_f-1} G_{x-y}(i) \log \{G_{x-y}(i)\} \quad (13)$$

$$DV = \text{Variance of } G_{x-y} \quad (14)$$

$$I1 = \frac{KXY - KXY1}{\max\{KX, KY\}} \quad (15)$$

$$I2 = \sqrt{(1 - \exp[-2.0[KXY2 - KXY]])} \quad (16)$$

$$KXY = -\sum_i \sum_j G_{ij} \log_2 G_{ij} \quad (17)$$

$$KXY1 = -\sum_i \sum_j G_{ij} \log_2 \{G_x(i)G_y(j)\} \quad (18)$$

$$KXY2 = -\sum_i \sum_j G_x(i)G_y(j) \log_2 \{G_x(i)G_y(j)\} \quad (19)$$

$$MCC = \sum_k \frac{G(i,k)G(j,k)}{G_x(i)G_y(k)} \quad (20)$$

GRLM (Radhakrishnan and Kuttiannan, 2012): It is considered as a matrix, in which the texture evaluation derives the texture features. The GLRM reveals higher-order statistical information by enhancing the image intensity. The computation of short-run emphasis, gray level non-uniformity, long-run emphasis, run percentage, run-length non-uniformity, HGRE and LGRE is given in equation (21) to equation (27), respectively. Here $Q(i,j)$ is the second-order joint conditional probability density function.

$$S^{RE} = \frac{1}{n} \sum_{i,j} \frac{Q(i,j)}{j^2} \quad (21)$$

$$G^{LN} = \frac{1}{n} \sum_i \left(\sum_j Q(i,j)^2 \right) \quad (22)$$

$$L^{RE} = \frac{1}{n} \sum_{i,j} j^2 Q(i,j) \quad (23)$$

$$R^P = \sum_{i,j} \frac{n_l}{Q(i,j)j} \quad (24)$$

$$R^{LN} = \frac{1}{n} \sum_i \left(\sum_j Q(i,j)^2 \right) \quad (25)$$

$$HG^{RE} = \frac{1}{n} \sum_{ij} i^2 Q(i, j) \quad (26) \quad \text{Segmentation for breast cancer detection}$$

$$LG^{RE} = \frac{1}{n} \sum_{ij} \frac{Q(i, j)}{i^2} \quad (27)$$

Thus, the combination of both GLCM and GLRM obtained finally can be represented as S_u , $u = 1, 2, \dots, N_U$, and N_U refers to the total number of features.

191

4. Proposed breast cancer detection model: optimized fuzzy classifier with proposed objective model

4.1 Proposed architecture with objective model

The developed breast cancer diagnosis model is diagrammatically shown in Figure 1, which consists of four main steps, like image pre-processing, tumor segmentation, feature extraction, and classification. In order to remove noise from the image, a filtering type termed as median filtering is applied in the pre-processing stage. Further, the segmentation process starts with the help of the optimized region growing algorithm. Once the tumor is segmented by the optimized region growing algorithm, few relevant feature sets like GLCM and GLRM are extracted. Some of the GLCM features are contrast, energy, entropy, homogeneity, variance, sum average, correlation, sum variance, sum entropy, difference entropy, difference variance, and information measures of correlation. Some of the GLRM features are short run emphasis, grey level non uniformity, long run emphasis, run percentage, run length non uniformity, high grey level run emphasis, and low grey level run emphasis.

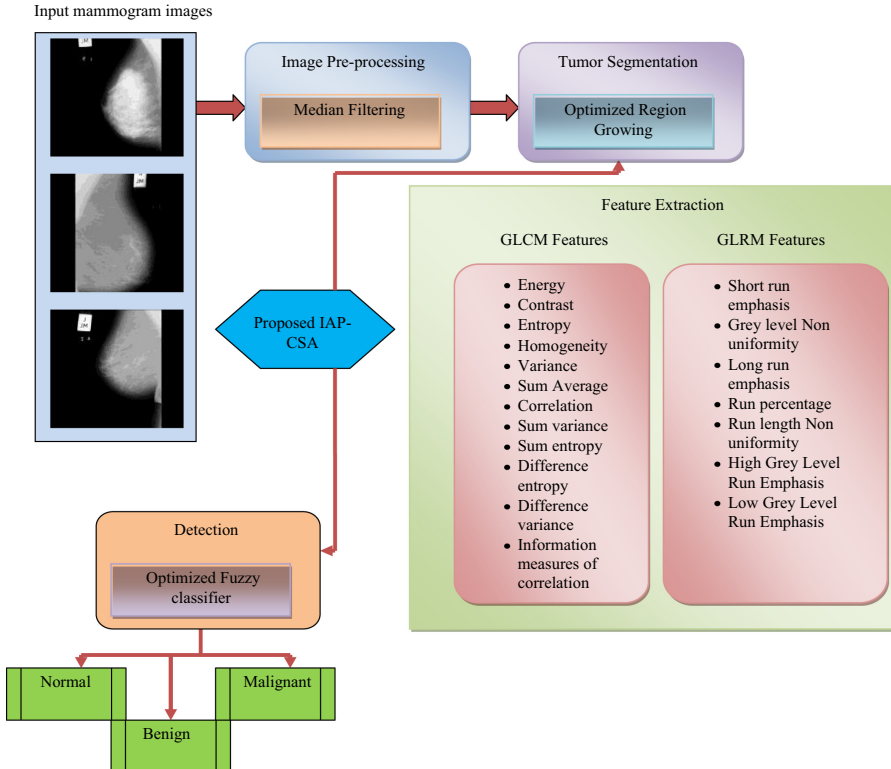


Figure 1. Architecture diagram of proposed breast cancer diagnosis model

variance, IMC1, IMC2, maximum correlation coefficient, etc., and GLRM features are gray level non-uniformity, long run emphasis, run percentage, run-length non-uniformity, HGRE, LGRE, etc. Finally, the classification stage uses the optimized Fuzzy classifier for categorizing the image into three classes like normal, benign, and malignant.

The novelty of the work is focussed on tumor segmentation and classification phase. In segmentation, the optimized region growing is used, whereas in the classification phase, an optimized Fuzzy classifier is used. The tolerance of region growing algorithm is optimized by a proposed meta-heuristic algorithm termed as IAP-CSA, in such a way that the segmentation accuracy is maximum. Moreover, the same algorithm IAP-CSA put its benefits on optimizing the membership function by tuning the membership limits.

Hereunder, the objective model of the proposed breast cancer detection model is given.

- (1) The first objective is to maximize the segmentation accuracy by comparing the segmented tumor part with the ground truth image. This objective is evaluated in the proposed IAP-CSA processed inside the region, growing for optimizing the tolerance value.
- (2) The second objective is to maximize the classification accuracy from the optimized fuzzy classifier. Here, the optimized membership function enhances the classification performance.

The mathematical equation to determine the accuracy B is represented in [equation \(28\)](#).

$$B = \frac{T^P + T^N}{T^P + T^N + F^P + F^N} \quad (28)$$

In [equation \(28\)](#), the variables T^P , T^N , F^P , and F^N specify the true positive, true negative, false positive and false negative elements, respectively.

4.2 Optimized fuzzy classifier-based detection

The detection or classification phase uses an optimized fuzzy classifier for differentiating the normal, benign and malignant images using the input features $S_u = S_1, S_2, \dots, S_{N_U}$. The main advantage of a fuzzy classifier ([Sousa et al., 2019](#)) is that the fuzzy set theory could express and manipulate the ambiguity and uncertainty. The initial process of the conventional fuzzy classifier is to generate the rules, and here, the exact categorization of images is generated by the triangular membership function, which is represented in [equation \(29\)](#).

$$\mu_H(Y) = \begin{cases} 0, & y \leq \text{low} \\ \frac{y - \text{low}}{\text{medium} - \text{low}}, & \text{low} < y \leq \text{medium} \\ \frac{\text{high} - y}{\text{high} - \text{medium}}, & \text{medium} < y < \text{high} \\ 0, & y \geq \text{high} \end{cases} \quad (29)$$

The membership function H is denoted as $\mu_H(Y)$ and high, low and medium are high, low, and medium operators. Here, Y indicates the universe of discourse and y is the concerned element of Y . The diagrammatic representation of the triangular membership function is shown in [Figure 2](#).

Let $\hat{r}_1 = \{S_u, O^i\}$, where O^i indicates the output in a specified range. In [equation \(30\)](#), the limiting factor δ_1 is provided and M_L refers to the number of linguistic variables.

$$\delta_1 = \max(\hat{r}_1) - \min(\hat{r}_1) \quad (30)$$

$$\delta'_1 = \frac{\delta_1}{M_L} \quad (31)$$

The maximum and minimum limit of linguistic variables is shown in equations (32), (33) and (34), respectively.

$$\begin{aligned} Low^{\min} &= \min(\hat{r}_1) \\ Low^{\max} &= \min(\hat{r}_1) + \delta'_1 \end{aligned} \quad (32)$$

$$\begin{aligned} medium^{\min} &= Low^{\max} + 0.1 \\ medium^{\max} &= \min(\hat{r}_1) + 2\delta'_1 \end{aligned} \quad (33)$$

$$\begin{aligned} High^{\min} &= \min(\hat{r}_1) + 2\delta'_1 + 0.1 \\ High^{\max} &= \max(\hat{r}_1) \end{aligned} \quad (34)$$

Since the limits of membership function play a vital role in determining the output degree, it is required to tune it properly. Hence, this paper uses the proposed IAP-CSA to optimize the membership limits, which have a positive effect on the final membership function. Here, it categorizes the output into three classes, i.e. normal, benign or malignant.

4.3 Encoding procedure

As mentioned earlier, the new contribution to segmentation, as well as the classification is provided here for automatic breast cancer detection. Hence, the solution to the proposed IAP-CSA optimization includes the tolerance from region growing, and the membership limits of a fuzzy classifier to maximize the segmentation, and detection accuracy. Accordingly, the solution encoding for tolerance and membership limits is shown in Figure 3.

4.4 Conventional CSA

The proposed IAP-CSA is used for optimizing region growing and fuzzy classifiers. The main inspiration of conventional CSA (Askarzadeh, 2016) is based on the food searching behavior of crows, which has already stored in hiding places. The algorithm focuses on a group of intelligent birds or crows. Crows will watch where the other birds are storing the food and rob it when the owner left the food. The main beliefs of CSA are mentioned below:

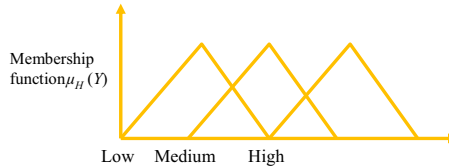


Figure 2.
The pattern of
triangular membership
function



Figure 3.
Solution encoding for
tolerance and
membership limits

- (1) Crows exist in the structure of flock.
- (2) Crows remember the concealing locations.
- (3) Crows follow each other for stealing.
- (4) Crows save the collection from stealing with a probability.

It is considered that there is d -dimensional space consists of the count of crows, and the location of the crow p at a time it in the search area is defined by a vector $X^{p,it}$ ($p = 1, 2, \dots, N; it = 1, 2, \dots, it_{\max}$), where $X^{p,it} = [X_1^{p,it}, X_2^{p,it}, \dots, X_d^{p,it}]$, and it_{\max} represents the maximum count of iterations. Every crow remembers the location of its hiding place. The location of hiding position of the crow p in time it is denoted by $h^{p,it}$ that is the best position of the crow has achieved. In iteration it , the crow q likes to see the concealing location that is represented by $h^{q,it}$. At that time, the crow p plans to follow the crow q to move towards the hiding location of crow q . At that point, two phases may occur:

- (1) Crow q doesn't know that crow p is following it. In this phase, the novel position of crow p is achieved as shown in equation (35), where rn_p be the random number with a uniform distribution between 0 and 1 and $lf^{p,it}$ represents the flight length of the crow p at it iteration.

$$X^{p,it+1} = X^{p,it} + rn_p \times lf^{p,it} \times (h^{q,it} - X^{p,it}) \quad (35)$$

- (2) Crow q knows that crow p is following it. In this case, crow q fools crow p by moving towards other locations of search space. The two phases are denoted in equation (36), where $AP^{q,it}$ indicates the awareness probability of crow q at time it .

$$X^{p,it+1} = \begin{cases} X^{p,it} + rn_p \times lf^{p,it} \times (h^{q,it} - X^{p,it}) & \text{if } rn_q \geq AP^{q,it} \\ \text{a random location} & \text{otherwise} \end{cases} \quad (36)$$

The process for implementing CSA is as follows:

- (1) To optimize the problem, decision variables and the concerned states are demonstrated. Next, the required measurable factors of CSA (N, it, lf, AP) are evaluated.
- (2) N crows are randomly placed in d -dimensional search space. Each crow represents an optimal solution is given by equation (37), where dv is the number of decision variables. Moreover, it is required to initialize the memory of each crow based on equation (38), since the crows do not have any experience before.

$$\text{Crows} = \begin{bmatrix} X_1^1 & X_2^1 & \Lambda & X_{dv}^1 \\ X_1^1 & x_2^2 & \Lambda & X_{dv}^2 \\ M & M & M & M \\ X_1^N & X_2^N & \Lambda & X_{dv}^N \end{bmatrix} \quad (37)$$

$$\text{Memory} = \begin{bmatrix} h_1^1 & h_2^1 & \Lambda & h_{dv}^1 \\ h_1^2 & h_2^2 & \Lambda & h_{dv}^2 \\ M & M & M & M \\ h_1^N & h_2^N & \Lambda & h_{dv}^N \end{bmatrix} \quad (38)$$

- (3) The quality of each crow's located point is calculated by placing the values of decision variables into fitness function.
- (4) Crows create a new position in the search space. The crow randomly picks one from the group and follows to locate the hidden foods by other crows. The new position of the crow is attained in [equation \(36\)](#).
- (5) The feasibility of crow's new location is evaluated. If it is optimal, then the crow updates its position, or else it remains in the current location.
- (6) Calculate the objective function for the new location of every crow.
- (g) Update the crow's memory by using [equation \(39\)](#), where $F(\cdot)$ indicates the fitness value.

$$h^{p,it+1} = \begin{cases} X^{p,it+1} & \text{if } f(X^{p,it+1}) \text{ is better than } F(h^{p,it}) \\ h^{p,it} & \text{Otherwise} \end{cases} \quad (39)$$

- (7) At the time of the termination criterion, the best position of the memory regarding the value of objective function is termed as the optimal solution.

The pseudo-code of conventional CSA is given in Algorithm 1.

Algorithm 1: Pseudo-code of Conventional CSA
Initialize the position of N crows Perform Fitness Evaluation Do memory initialization While $it < it_{\max}$ For $1 : N$ Select a single crow randomly Fix awareness probability as 0.1 If $m_q \geq AP^{q,it}$ Compute the position of a crow using Eq. (35) else Select a random position End if End for Check the prospect of new positions Perform Fitness Evaluation Do memory updates using Eq. (39) End while

4.5 Proposed IAP-CSA in segmentation and classification

Although the conventional CSA offers interesting beneficial characteristics, the searching strategy still faces a few difficulties, while solving high multi-modal functions. Hence in order to resolve the compound optimization problems considered in segmentation as well as classification, a new version of CSA termed as IAP-CSA has been introduced in this paper. The improvement is made on awareness probability, which is fixed as 0.1 in conventional CSA ([Askarzadeh, 2016](#)). Here in the proposed IAP-CSA, the computation of awareness probability is based on [equation \(40\)](#).

$$AP = \text{rand} \times \frac{F_{it}}{F_{it}^M} \tag{40}$$

In [equation \(40\)](#), the variable `rand` refers to a random number between 0 and 1, F_{it} indicates the fitness value of the current solution, and F_{it}^M indicates the average of all fitness values. The pseudo-code of the proposed IAP-CSA is given in [Algorithm 2](#).

Algorithm 2: Pseudo-code of proposed IAP-CSA
Initialize the position of N crows
Perform Fitness Evaluation
Do memory initialization
While $it < it_{\max}$
 For $1 : N$
 Select a single crow randomly
 Compute awareness probability using Eq. (40)
 If $rn_q \geq AP^{q,it}$
 Compute the position of a crow using Eq. (35)
 else
 Select a random position
 End if
 End for
 Check the prospect of new positions
 Perform Fitness Evaluation
 Do memory updates using Eq. (39)
End while

The overall process for optimized segmentation and classification based IAP-CSA is shown in [Figure 4](#).

5. Results and discussions

5.1 Experimental setup

The developed breast cancer detection model using mammogram images was implemented in MATLAB 2018a, and the analysis was done. The mammogram dataset used for the experimentation was downloaded from the URL (<https://www.kaggle.com/kmader/mias-mammography>; Access data 2019-09-10). Here, a totally 325 images were used, which includes normal, benign as well as malignant images. During the analysis, the performance metrics like accuracy, sensitivity, specificity, precision, NPV, F1-score and MCC and negative measures such as FPR, FNR, and FDR were evaluated for both segmentation and classification. [Table 2](#) shows the list of parameters used in the proposed algorithm. Here, the total population size of the experiment was taken as 10, the total iteration for segmentation was 25, and the total iteration for classification was 100.

5.2 Performance metrics

In this paper, ten performance measures are taken into consideration for segmentation and classification analysis. They are shown below:

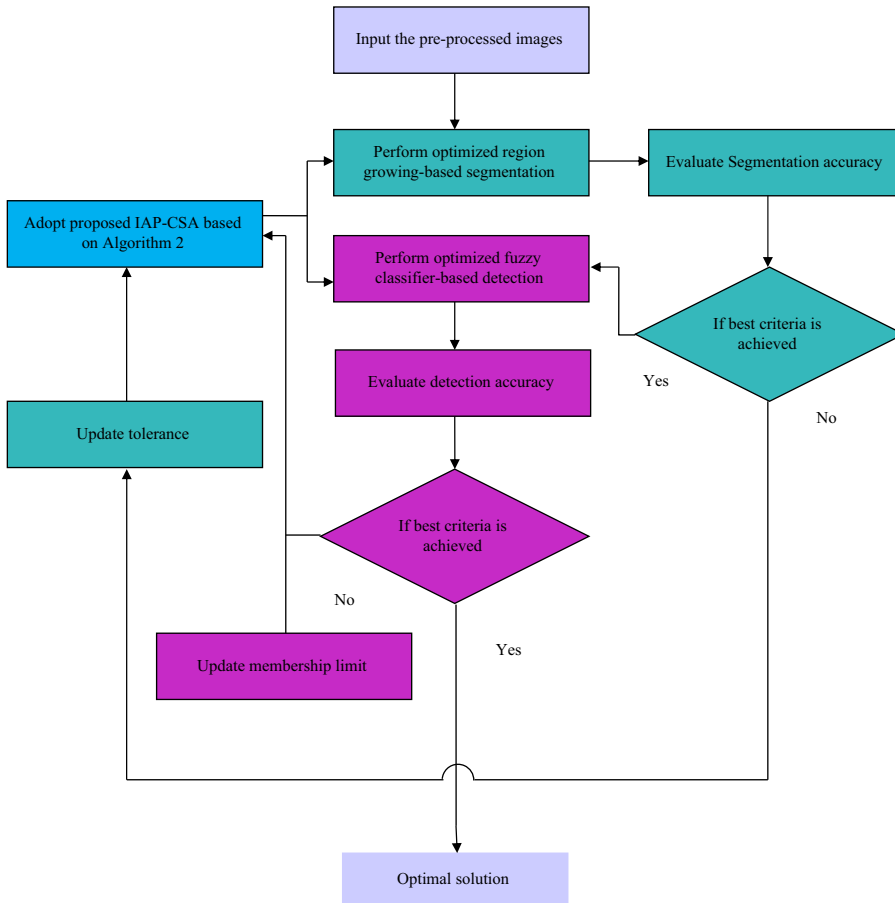


Figure 4.
Flow chart
representation of
optimized breast
cancer detection

Parameters	Values
Population size	10
Maximum number of iterations for segmentation	25
Maximum number of iterations for classification	100
Awareness probability of IAP-CSA	0.1
Flight length of IAP-CSA	2

Table 2.
List of parameters

- (1) Accuracy: It is a “ratio of the observation of exactly predicted to the whole observations.” The formula for accuracy is shown in [equation \(28\)](#).
- (2) Sensitivity: It measures “the number of true positives, which are recognized exactly.” It is mathematically represented in [equation \(41\)](#)

$$Se = \frac{T^P}{T^P + F^N} \quad (41)$$

- (3) Specificity: It measures “the number of true negatives, which are determined precisely.” The specificity is formulated as [equation \(42\)](#).

$$Sp = \frac{T^N}{F^P} \quad (42)$$

- (4) Precision: It is “the ratio of positive observations that are predicted exactly to the total number of observations that are positively predicted.” It is shown in [equation \(43\)](#).

$$Pr = \frac{T^P}{T^P + F^P} \quad (43)$$

- (5) FPR: It is computed as “the ratio of the count of false-positive predictions to the entire count of negative predictions.” FPR is numerically represented in [equation \(44\)](#).

$$FPR = \frac{F^P}{F^P + T^N} \quad (44)$$

- (6) FNR: It is “the proportion of positives which yield negative test outcomes with the test.” It is numerically denoted in [equation \(45\)](#).

$$FNR = \frac{F^N}{F^N + T^P} \quad (45)$$

- (7) NPV: It is the ratio of incorrectly recognized negative observations of the total number of negative observations. It is represented in [equation \(46\)](#).

$$NPV = \frac{F^N}{F^N + T^N} \quad (46)$$

- (8) FDR: It is the number of false positives in all of the rejected hypotheses. The formula for FDR is shown in [equation \(47\)](#).

$$FDR = \frac{F^P}{F^P + T^P} \quad (47)$$

- (9) F1 score: It is defined as “the harmonic mean between precision and recall. It is used as a statistical measure to rate performance.” It is numerically shown in [equation \(48\)](#).

$$F1score = \frac{Se \times Pr}{Pr + Se} \quad (48)$$

- (10) MCC: “It is a correlation coefficient computed by four values,” as denoted in [equation \(49\)](#).

$$MCC = \frac{T^P \times T^N - F^P \times F^N}{\sqrt{(T^P + F^P)(T^P + F^N)(T^N + F^P)(T^N + F^N)}} \quad (49)$$

5.3 Segmentation performance

This part of the paper concentrates on the analysis of segmentation that is enhanced using the IAP-CSA-based region growing. The developed IAP-CSA is compared with the

conventional PSO, GWO, WOA and CSA-based region growing to analyze the performance of the introduced system. The results of the segmented images by the suggested IAP-CSA region growing with the conventional algorithms are shown in Figure 5. Moreover, the overall segmentation analysis is shown in Table 3. Here, the accuracy of the proposed IAP-CSA is producing the best accuracy for correctly categorizing the regions. The developed IAP-CSA is 15.7% better than conventional region growing, 0.968% better than PSO and CSA, 1% better than GWO, and WOA-based region growing algorithms. The sensitivity of the suggested IAP-CSA recognizes the true positives exactly. Moreover, the introduced IAP-CSA is 80% improved than the existing region growing, 60.27% improved than PSO, 62.3% improved than GWO, 62.1% improved than WOA, and 60.2% improved than CSA in terms of sensitivity. Along with these, other performance measures also produce the best outcomes for the developed IAP-CSA when compared to existing algorithms. Hence, it can be confirmed that the developed system has the best segmentation performance over state-of-the-other optimized models.

5.4 Performance analysis

In this context, the whole performance of the proposed IAP-CSA-based fuzzy classifier is evaluated based on other optimized fuzzy classifiers, which is graphically shown in Figure 6, and the overall performance is shown in Table 4. The performance of the IAP-CSA-fuzzy is compared with the existing PSO-fuzzy, GWO-fuzzy, WOA-fuzzy, and CSA-fuzzy concerning various learning percentages. From Figure 6a, the accuracy of the suggested IAP-CSA-fuzzy is identified exactly overall learning percentages. It is 28.9% better than the existing Fuzzy at 85% learning percentage. Also, the sensitivity of the proposed IAP-CSA-fuzzy is exactly recognized as the true positives at all learning percentages. Now, at 75% learning percentage the sensitivity of the recommended IAP-CSA-fuzzy is 2.32% enhanced than the existing Fuzzy, 4.76% enhanced than GWO, and 6.02% enhanced than the CSA-based fuzzy classifiers as shown in Figure 6b. In Figure 6c, the specificity of the developed IAP-CSA has precisely identified the true negatives overall learning percentages. For the specificity at 65% learning percentage, the introduced IAP-CSA-fuzzy is 1.19%, and 70% improved than GWO, and fuzzy, respectively. Moreover, the precision of the offered IAP-CSA-based fuzzy has predicted the positive observations in all learning percentages that is shown in Figure 6d. Considering the learning percentage as 75%, the precision of the developed IAP-CSA-fuzzy is 6.25% improved than CSA, and 70% improved than fuzzy. Additionally, the FPR of the IAP-CSA-fuzzy is exactly calculating the false-negative predictions among whole learning percentages. From Figure 6e, the FPR at 85% learning percentage the proposed IAP-CSA, is 88.57% superior to fuzzy. Along with these, the FNR of the suggested IAP-CSA has resulted in the negative from the positive predictions at all learning percentages. In Figure 6f, at 75% learning percentage, the FNR of the developed IAP-CSA-fuzzy is 14.28%, 20% and 25% better than fuzzy, GWO and CSA-based fuzzy systems, respectively. Further, the NPV of the proposed IAP-CSA has not recognized the negative observation's overall learning percentages. At learning percentage 85%, from Figure 6g, the NPV of the recommended IAP-CSA-fuzzy is 50.7% improved than fuzzy. From Figure 6h, FDR of the suggested IAP-CSA-fuzzy produced the number of false positives from the rejected observations overall learning percentages. Now at 75% learning percentage, the FDR of the proposed IAP-CSA is 40% superior to CSA and 76.92% superior to fuzzy. In Figure 6i, the F1 score of the proposed IAP-CSA is determined by calculating the mean between sensitivity and the precision at all learning percentages. For now, the F1 score of the recommended IAP-CSA-fuzzy is 2.73% improved than GWO, 4.16% improved than WOA, and 7.14% improved than CSA-based

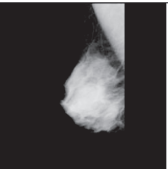
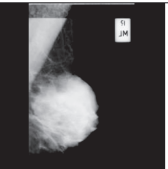
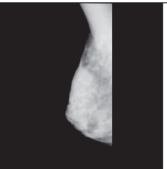
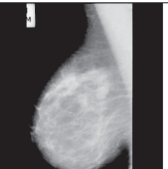
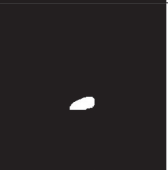
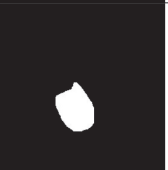
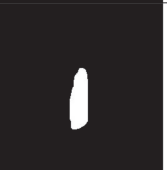
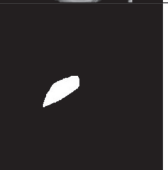




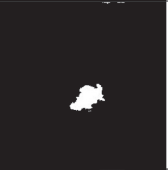












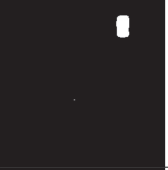
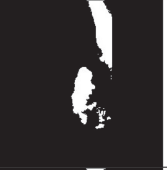





Methods				
Ground truth images				
Region Growing				
PSO-Region Growing				
GWO-Region Growing				
WOA-Region Growing				
CSA-Region Growing				
IAP-CSA-Region Growing				

Figure 5. Segmentation results for proposed and conventional region growing (a) Image 1 (b) Image 2, (c) Image 3, and (d) Image 4

Performance metrics	Segmentation for breast cancer detection					
	Region growing (Feng <i>et al.</i> , 2018)	PSO – region growing (Pedersen and Chipperfield, 2010)	GWO – region growing (Mirjalili <i>et al.</i> , 2014)	WOA – region growing (Mirjalili and Lewis, 2016)	CSA – region growing (Askarzadeh, 2016)	IAP-CSA – region growing
“Accuracy”	0.84781	0.97157	0.97121	0.97123	0.97157	0.98098
“Sensitivity”	0.12029	0.37953	0.37478	0.37507	0.3796	0.60829
“Specificity”	0.99805	0.98727	0.98732	0.98732	0.98727	0.98653
“Precision”	0.9272	0.44167	0.44396	0.44392	0.44167	0.40253
“FPR”	0.00195	0.012727	0.012681	0.012681	0.012727	0.013465
“FNR”	0.87971	0.62047	0.62522	0.62493	0.6204	0.39171
“NPV”	0.99805	0.98727	0.98732	0.98732	0.98727	0.98653
“FDR”	0.0728	0.55833	0.55604	0.55608	0.55833	0.59747
“F1-score”	0.21295	0.40825	0.40645	0.4066	0.40829	0.48447
“MCC”	0.30249	0.39496	0.39328	0.39343	0.39499	0.48573

201

Table 3.
Analysis of proposed and conventional segmentation performance

fuzzy systems. Moreover, the MCC of the introduced IAP-CSA-fuzzy is computed at all learning percentages produced the best, and it is shown in Figure 6j. At 55% learning percentage, the MCC of the developed IAP-CSA-fuzzy is 8.33% enhanced than CSA, 10.16% enhanced than GWO, and 85.7% enhanced than fuzzy. Moreover, from Table 4, the accuracy of the proposed IAP-CSA-fuzzy is 41.9% improved than the fuzzy classifier, 2.80% improved than PSO, WOA, and CSA, and 2.32% improved than GWO-based fuzzy classifiers. Additionally, the specificity of the introduced IAP-CSA is 75.29% superior to the fuzzy classifier, 2.05% superior to PSO, GWO, WOA and CSA. Hence, it is confirmed that the introduced IAP-CSA-fuzzy is effective for automatic recognition of breast cancer from the determined observations.

5.5 Comparison with existing classifiers

The implemented IAP-CSA-Fuzzy is compared with the conventional classifiers, such as NN (Yildiz *et al.*, 2019), SVM (Yu *et al.*, 2015) and Fuzzy (Sousa *et al.*, 2019). The comparison results are shown in Table 5. From Table 5, the accuracy of the introduced IAP-CSA-Fuzzy is determined precisely, that is, 9.54% superior to NN, 35.8% superior to SVM, and 41.9% superior to the fuzzy classifier. Additionally, the precision of the implemented IAP-CSA-Fuzzy is 2.45% enhanced than NN, 68.9% enhanced than SVM, and 79.3% enhanced than fuzzy. Therefore, the performance of the IAP-CSA-Fuzzy outperformed the state-of-the-art classifiers.

5.6 Practical implications

Mammogram image segmentation is useful in detecting the breast cancer regions. The proposed breast cancer detection model uses the mammogram images, hence it helps better diagnosis. The proposed method detects only tumor regions from the original input image successfully. Moreover, the proposed breast cancer detection reduces the treatment and time spent for recovery. The proposed breast cancer detection model helps to find minimally invasive therapy to make better results and reduce side effects. The proposed model provides the supplementary information used to improve staging and therapy planning. Also, it helps to reduce the mortality of patients with breast cancer.

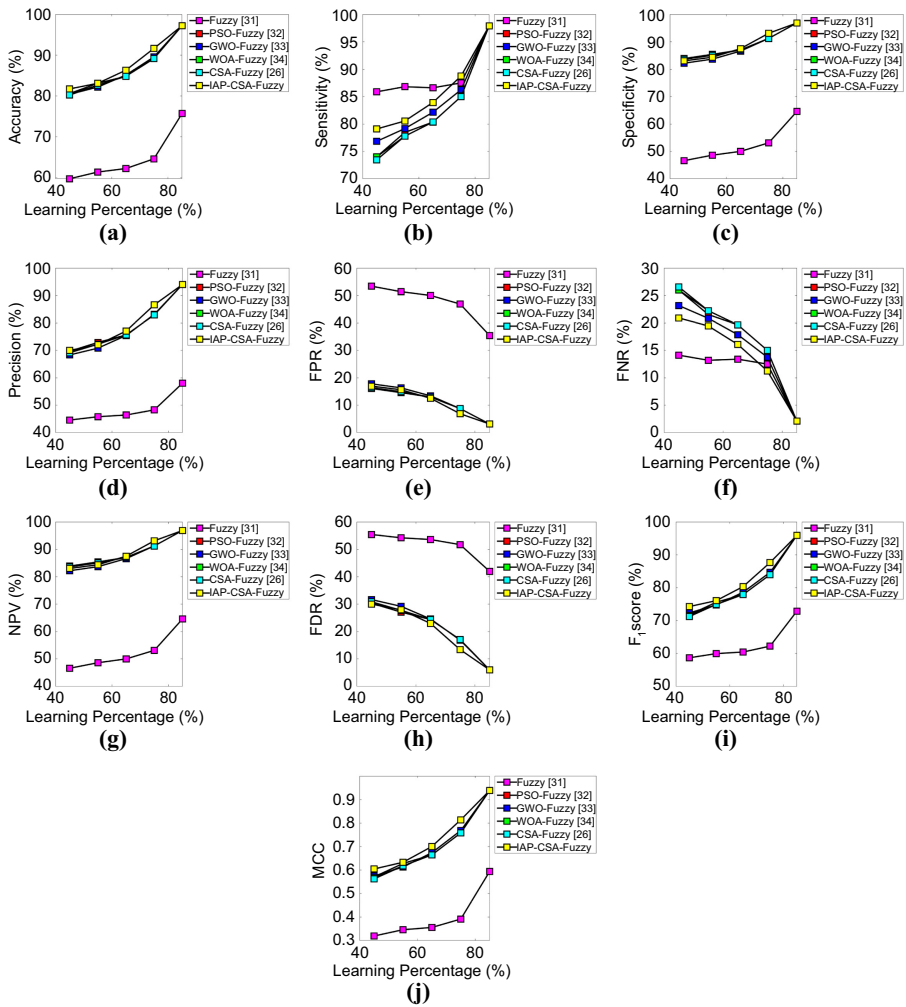


Figure 6. Performance analysis of proposed and existing algorithms for breast cancer detection: (a) accuracy, (b) sensitivity, (c) specificity, (d) precision, (e) FPR, (f) FNR, (g) NPV, (h) FDR, (i) F1-score and (j) MCC

6. Conclusion

The implemented automatic breast cancer detection process consisted of four phases: pre-processing, segmentation, feature extraction and classification. At first, the median filter was used for pre-processing, which was performed to eliminate the noise from the image. In the segmentation phase, an optimized region growing algorithm was used, whereas the classification phase has utilized the optimized fuzzy logic classifier. The input feature supplied to the classifier was GLRM, and GLCM sets. In the proposed model, the tolerance of region growing, and the membership function of the fuzzy logic classifier was optimized by the proposed IAP-CSA algorithms, which was the improved version of the existing CSA. The performance analysis was done for both segmentation and classification. From the analysis, the accuracy of the proposed IAP-CSA-based fuzzy was 41.9% improved than the fuzzy classifier, 2.80% improved than PSO, WOA, and CSA, and 2.32% improved than GWO-based

Performance metrics	Segmentation for breast cancer detection					
	Fuzzy (Sousa <i>et al.</i> , 2019)	PSO- fuzzy (Pedersen and Chipperfield, 2010)	GWO- fuzzy (Mirjalili <i>et al.</i> , 2014)	WOA- fuzzy (Mirjalili and Lewis, 2016)	CSA- fuzzy (Askarzadeh, 2016)	IAP- CSA- fuzzy
"Accuracy"	0.64583	0.89167	0.89583	0.89167	0.89167	0.91667
"Sensitivity"	0.875	0.85	0.8625	0.85	0.85	0.8875
"Specificity"	0.53125	0.9125	0.9125	0.9125	0.9125	0.93125
"Precision"	0.48276	0.82927	0.83133	0.82927	0.82927	0.86585
"FPR"	0.46875	0.0875	0.0875	0.0875	0.0875	0.06875
"FNR"	0.125	0.15	0.1375	0.15	0.15	0.1125
"NPV"	0.53125	0.9125	0.9125	0.9125	0.9125	0.93125
"FDR"	0.51724	0.17073	0.16867	0.17073	0.17073	0.13415
"F1-score"	0.62222	0.83951	0.84663	0.83951	0.83951	0.87654
"MCC"	0.39161	0.7579	0.7681	0.7579	0.7579	0.81381

203

Table 4.
Overall performance of optimized breast cancer diagnosis

Performance metrics	Performance of proposed optimized fuzzy classifier over conventional classifiers			
	NN (Yildiz <i>et al.</i> , 2019)	SVM (Yu <i>et al.</i> , 2015)	Fuzzy (Sousa <i>et al.</i> , 2019)	IAP-CSA- fuzzy
"Accuracy"	0.83681	0.675	0.64583	0.91667
"Sensitivity"	0.625	0.36458	0.875	0.8875
"Specificity"	0.94271	0.7526	0.53125	0.93125
"Precision"	0.84507	0.26923	0.48276	0.86585
"FPR"	0.057292	0.2474	0.46875	0.06875
"FNR"	0.375	0.63542	0.125	0.1125
"NPV"	0.94271	0.7526	0.53125	0.93125
"FDR"	0.15493	0.73077	0.51724	0.13415
"F1-score"	0.71856	0.30973	0.62222	0.87654
"MCC"	0.62094	0.10548	0.39161	0.81381

fuzzy classifiers. Additionally, the accuracy of the developed IAP-CSA-fuzzy was 9.54% better than NN, 35.8% better than SVM, and 41.9% better than the existing fuzzy classifier. Hence, it is concluded that the implemented breast cancer detection model was efficient in determining the normal, benign and malignant images.

References

- Al-antari, M.A., Al-masni, M.A., Choi, M., Han, S.-M. and Kim, T.-S. (2018), "A fully integrated computer-aided diagnosis system for digital X-ray mammograms via deep learning detection, segmentation, and classification", *International Journal of Medical Informatics*, Vol. 117, pp. 44-54.
- Askarzadeh, A. (2016), "A novel metaheuristic method for solving constrained engineering optimization problems: crow search algorithm", *Computers and Structures*, Vol. 169, pp. 1-12.
- Bhosle, U. and Deshmukh, J. (2018), "Mammogram classification using AdaBoost with RBF SVM and Hybrid KNN-RBF SVM as base estimator by adaptively adjusting γ and C value", *International Journal of Information Technology*, pp. 1-8.
- Dietterich, T.G. (2000), "An experimental comparison of three methods for constructing ensembles of decision trees: bagging, boosting, and randomization", *Machine Learning*, Vol. 40 No. 2, pp. 139-157.
- Duraisamy, S. and Emperumal, S. (2017), "Computer-aided mammogram diagnosis system using deep learning convolutional fully complex-valued relaxation neural network classifier", *IET Computer Vision*, Vol. 11 No. 8, pp. 656-662.

- Fan, M., Li, Y., Zheng, S., Peng, W., Tang, W. and Li, L. (2019), "Computer-aided detection of mass in digital breast tomosynthesis using a faster region-based convolutional neural network", *Methods*.
- Feng, Q., Gao, B., Lu, P., Woo, W.L., Yang, Y., Fan, Y., Qiu, X. and Gu, L. (2018), "Automatic seeded region growing for thermography debonding detection of CFRP", *NDT and E International*, Vol. 99, pp. 36-49.
- Freund, Y. and Schapire, R.E. (1997), "A decision-theoretic generalization of on-line learning and an application to boosting", *Journal of Computer and System Sciences*, Vol. 55 No. 1, pp. 119-139.
- Hellquist, B.N., Duffy, S.W., Abdsaleh, S., Björneld, L., Bordás, P., Tabár, L., Viták, B., Zackrisson, S., Nyström, L. and Jonsson, H. (2010), "Effectiveness of population-based service screening with mammography for women ages 40 to 49 years", *Cancer*, Vol. 117 No. 4, pp. 714-722.
- Herent, P., Schmauch, B., Jehanno, P., Dehaene, O., Saillard, C., Balleyguier, C., Arfi-Rouche, J. and Jégou, S. (2019), "Detection and characterization of MRI breast lesions using deep learning", *Diagnostic and Interventional Imaging*, Vol. 100 No. 4, pp. 219-225.
- Jasbi, P., Wang, D., Cheng, S.L., Fei, Q., Cui, J.Y., Liu, L., Wei, Y., Raftery, D. and Gu, H. (2019), "Breast cancer detection using targeted plasma metabolomics", *Journal of Chromatography*, Vol. 1105, pp. 26-37.
- Khan, S.U., Islam, N., Jan, Z., Din, I.U. and Joel C.Rodrigues, J.P. (2019), "A novel deep learning-based framework for the detection and classification of breast cancer using transfer learning", *Pattern Recognition Letters*, Vol. 125, pp. 1-6.
- Kim, J., Cho, H., Gwak, G., Yang, K., Kim, J.Y., Shin, Y.J., Seo, Y.Y. and Park, I. (2019), "Factors affecting the negative predictive value of positron emission tomography/computed tomography for axillary lymph node staging in breast cancer patients", *Asian Journal of Surgery*.
- Kopans, D.B. (2013), "Digital breast tomosynthesis: a better mammogram", *Radiology*, Vol. 267 No. 3.
- Kuncheva, L. and Whitaker, C.J. (2002), "Using diversity with three variants of boosting: aggressive, conservative, and inverse", *Multiple Classifier Systems*, pp. 81-90.
- Li, H., Zhuang, S., Li, D., Zhao, J. and Ma, Y. (2019), "Benign and malignant classification of mammogram images based on deep learning", *Biomedical Signal Processing and Control*, Vol. 51, pp. 347-354.
- Malegori, C., Franzetti, L., Guidetti, R., Casiraghi, E. and Rossi, R. (2016), "GLCM, an image analysis technique for early detection of biofilm", *Journal of Food Engineering*, Vol. 185, pp. 48-55.
- Menegaz, G.L. and Guimarães, G. (2019), "Development of a new technique for breast tumor detection based on thermal impedance and a damage metric", *Infrared Physics and Technology*, Vol. 97, pp. 401-410.
- Mirjalili, S. and Lewis, A. (2016), "The whale optimization algorithm", *Advances in Engineering Software*, Vol. 95, pp. 51-67.
- Mirjalili, S., Mirjalili, S.M. and Lewis, A. (2014), "Grey wolf optimizer", *Advances in Engineering Software*, Vol. 69, pp. 46-61.
- Nelson, H.D., Fu, R., Cantor, A., Pappas, M., Daeges, M. and Humphrey, L. (2016), "Effectiveness of breast cancer screening: systematic review and meta-analysis to update the 2009 U.S. Preventive services task force recommendation", *Annals of Internal Medicine*, Vol. 164 No. 4, pp. 244-255.
- Oliveira, J.E.E., Araújo, A.A. and Deserno, T.M. (2011), "Content-based image retrieval applied to BI-RADS tissue classification in screening mammography", *World Journal of Radiology*, Vol. 3 No. 1, pp. 24-31.
- Osman, N.M., Ghany, E.A. and Chalabi, N. (2018), "The added benefit of digital breast tomosynthesis in second breast cancer detection among treated breast cancer patients", *The Egyptian Journal of Radiology and Nuclear Medicine*, Vol. 49 No. 4, pp. 1182-1186.

-
- Pedersen, M.E.H. and Chipperfield, A.J. (2010), "Simplifying particle swarm optimization", *Applied Soft Computing*, Vol. 10 No. 2, pp. 618-628.
- Poorolajal, J., Akbari, M.E., Ziaee, F. and Karami, M. (2017), "Breast cancer screening (BCS) chart: a basic and preliminary model for making screening mammography more productive and efficient", *Journal of Public Health*, Vol. 40 No. 2, pp. 1-8.
- Qi, X., Zhang, L., Chen, Y., Pi, Y., Chen, Y., Lv, Q. and Yi, Z. (2019), "Automated diagnosis of breast ultrasonography images using deep neural networks", *Medical Image Analysis*, Vol. 52, pp. 185-198.
- Radhakrishnan, M. and Kuttiannan, T. (2012), "Comparative analysis of feature extraction methods for the classification of prostate cancer from TRUS medical images", *IJCSI International Journal of Computer Science Issues*, Vol. 9 No. 1.
- Schwenk, H. and Bengio, Y. (2000), "Boosting neural networks", *Neural Computation*, Vol. 12 No. 8, pp. 1869-1887.
- Seryasat, O.R. and Haddadnia, J. (2018), "Evaluation of a new ensemble learning framework for mass classification in mammograms", *Clinical Breast Cancer*, Vol. 18 No. 3, pp. e407-e420.
- Siegel, R.L., Miller, K.D. and Jemal, A. (2018), "Cancer statistics, 2018", *CA: A Cancer Journal for Clinicians*, Vol. 68, pp. 7-30.
- Sousa, M.J., Moutinho, A. and Almeida, M. (2019), "Classification of potential fire outbreaks: a fuzzy modeling approach based on thermal images", *Expert Systems with Applications*, Vol. 129, pp. 216-232.
- Vijayarajeswari, R., Parthasarathy, P., Vivekanandan, S. and Basha, A.A. (2019), "Classification of mammogram for early detection of breast cancer using SVM classifier and Hough transform", *Measurement*, Vol. 146, pp. 800-805.
- Yıldız, İ., Tian, P., Dy, J., Erdoğan, D., Brown, J., Kalpathy-Cramer, J., Ostmo, S., Campbell, J.P., Chiang, M.F. and Ioannidis, S. (2019), "Classification and comparison via neural networks", *Neural Networks*, Vol. 118, pp. 65-80.
- Yu, S., Tan, K.K., Sng, B.L., Shengjin and Sia, A.T.H. (2015), "Lumbar ultrasound image feature extraction and classification with Support vector machine", *Ultrasound in Medicine and Biology*, Vol. 41 No. 10, pp. 2677-2689.
- Zhang, X., Zhang, Y., Han, E.Y., Jacobs, N., Han, Q., Wang, X. and Liu, J. (2018), "Classification of whole mammogram and tomosynthesis images using deep convolutional neural networks", in *IEEE Transactions on NanoBioscience*, Vol. 17 No. 3, pp. 237-242.
- Zhu, Y. and Huang, C. (2012), "An improved median filtering algorithm for image noise reduction", *Physics Procedia*, Vol. 25, pp. 609-616.

Corresponding author

Rajeshwari S. Patil can be contacted at: rajeshwarispatil54@gmail.com